Metagenomics and Metatranscriptomics Reveal Pathway of 3-Chloroaniline Degradation in Wastewater Reactors

Hari Seshan[1,2,□,§], Ezequiel Santillan[1,2,§], Florentin Constancias[1], Uma Shankari Chandra Segaran[1], Rohan B. H. Williams[1] and Stefan Wuertz[1,2,3,*]

[1]Singapore Centre for Environmental Life Sciences Engineering, Nanyang Technological University, 637551, Singapore.

[2]Department of Civil and Environmental Engineering, University of California, Davis, CA 95616, U.S.A.

[3]School of Civil and Environmental Engineering, Nanyang Technological University, Singapore, 639798, Singapore.

*Correspondence to: Stefan Wuertz, swuertz@ntu.edu.sg

□ Current affiliation: Stantec Australia Pty Ltd, 52 Merivale St, South Brisbane QLD 4101, Australia.

[§]H.S. and E.S. contributed equally.

Abstract

Biological wastewater treatment systems are often affected by major shifts in influent quality, including the input of various toxic chemicals. Yet the mechanisms underlying adaptation of activated sludge process performance when challenged with a sustained toxin input have not been studied in a controlled and replicated experiment. Three replicate bench-scale bioreactors were subjected to a chemical disturbance in the form of 3-chloroaniline (3-CA) input over 132 days, following an acclimation period of 58 days, while three control reactors received no 3-CA input. The nitrification process was initially affected by 3-CA input; yet all three treatment reactors evolved to biologically degrade 3-CA within three weeks of the experiment, resulting in partial nitrification recovery. 16S rRNA amplicon sequencing revealed that ammonia oxidizers were initially impacted by 3-CA, and a new ammonia oxidizing community emerged with the onset of 3-CA degradation. Combining process and microbial community data from amplicon sequencing with potential functions gleaned from assembled metagenomics and metatranscriptomics data, 3-CA degradation was shown to likely occur via a phenol monooxygenase followed by ortho-cleavage of the aromatic ring. The relative abundance of genera *Gemmatimonas*, *Saprospiraceae OLB8* and *Taibaiella* correlated significantly with 3-CA degradation. This study demonstrated the impact of a sustained stress on the activated sludge community and wastewater treatment process and its subsequent recovery. Using a combination of techniques in a controlled and replicated experiment, we showed that microbial communities can evolve degradative capacity following a sustained xenobiotic input, specific functions like nitrification can fully or partially recover and targeted culture-independent approaches can be used to elucidate the mechanisms of adaptation.

1 Introduction

The activated sludge process in biological wastewater treatment involves a complex microbial community performing a range of metabolic functions under controlled conditions. Major shifts in process performance can occur when a disturbance or change is imposed on this microbial community. Such disturbances can be operational (Thompson *et al.*, 2006; Valipour *et al.* 2014, Santillan *et al.*, 2020), physical (Hwang *et al.*, 2006; Vargas *et al.*, 2013), or chemical (Kelly *et al.*, 2004; Falk and Wuertz, 2010). While short-term (or pulse) disturbances have been studied extensively (Boon *et al.*, 2000; Henriques *et al.*, 2007; Ma *et al.*, 2020), long-term (sustained) disturbances have not. Sustained disturbances provide an opportunity for processes to adapt and recover (Johnston *et al.*, 2019), and studying them mechanistically may help understand how to buffer against disruptions to the wastewater treatment process (Briones and Raskin, 2003).

Nitrification followed by denitrification is the conventional pathway for nitrogen removal from wastewater (Kuypers *et al.*, 2018). It frequently dictates footprint and energy use in biological wastewater treatment (McCarty *et al.*, 2011; Liu *et al.*, 2018), and is also a common candidate for process disruption (Siripong and Rittman, 2007), owing to its dependence on two interdependent groups of slow-growing autotrophs: ammonia oxidizing bacteria (AOB) and nitrite oxidizing bacteria (NOB). AOB maintain a stable population during long-term low-temperature periods, even when the nitrification process fails (Delatolla *et al.*, 2012; Johnston *et al.*, 2019). AOB were also shown to be more resistant and resilient than NOB under a sustained operational disturbance where the organic loading to replicate bioreactors was changed (Santillan *et al.* 2020b). The loss and subsequent recovery of nitrifiers have been seen when a solids retention time (SRT) reduction was imposed on a full-scale system (Vuono *et al.*, 2015), with a slight change in nitrifier community composition after the disturbance ended. After a pulse chemical disturbance in the form of 3-chloroaniline (3-CA), Ma *et al.* (2020) found that both AOB and NOB relative abundance decreased, but recovered within two weeks to pre-disturbance levels. Alves *et al.* (2017), however, only saw AOB recovery after a pulse phenol disturbance. Few studies have examined the impact of a sustained xenobiotic stress on nitrifiers in a controlled, replicated study.

The compound 3-chloroaniline (3-CA) is a by-product of the production of herbicides and azo dyes (Ficara and Rozzi, 2001). It disrupts nitrification by inhibiting AOB activity (McCarty, 1999; Falk and Wuertz, 2010).Its impact on wastewater treatment has been assessed in bench-scale systems using pulse inputs from 40 mg/L 3-CA (Ma *et al.*, 2020) to 250 mg/L 3-CA (Boon *et al.*, 2000), continuous inputs up to 120 mg/L 3-CA (Falk and

Wuertz, 2010; Zhu *et al.*, 2008), and recurring pulse inputs of 70 mg/L at varying frequencies (Santillan *et al.*, 2019). The biological degradation of 3-CA involves the conversion to a chlorocatechol, followed by the cleavage of the aromatic ring and channelling into TCA cycle intermediates (Reineke, 1999; Pimviriyakul *et al.*, 2019). Some of these studies saw 3-CA degradation (Zhu *et al.*, 2008; Santillan *et al.*, 2019), but none have attempted to determine the relevant pathway involved.

Metagenomic and metatranscriptomic analyses allow the examination of differential gene enrichment and transcription respectively, in complex microbial communities like activated sludge. Some researchers have used transcriptomics approaches to elucidate degradation pathways via gene transcription in aromatics degradation in pure culture experiments (Tam *et al.*, 2006; Yan and Wu, 2017; Cauduro *et al.*, 2020; Ma *et al.*, 2020b). Long-term metatranscriptomics sampling has also helped show differential enrichment and transcription of aromatics degradation genes in activated sludge bioreactors (Sato *et al.*, 2019; Sun *et al.*, 2019; Yu *et al.*, 2019). However, combining these methods with amplicon sequencing to determine degrading taxa and the likely degradation pathway in tandem with the degradation of the compound in question has not been attempted.

This study investigated the impact of a sustained xenobiotic disturbance in the form of 3-CA addition for 132 days on activated sludge wastewater treatment, focusing on nitrification and 3-CA degradation mechanisms. Of six bench-scale bioreactors that had been acclimated with activated sludge from a wastewater treatment plant, three received sustained 3-CA input and three were maintained as controls. We examined, through intensive nutrient cycling profiles, how the emergence of 3-CA degradation impacted process recovery and the nitrifier microbial community. The most likely taxa responsible for degradation of 3-CA and the most likely degradation pathway for 3-CA were determined using a combination of amplicon sequencing, metagenomics and metatranscriptomics.

2 Materials and methods

2.1 Experimental design

Six sequencing batch bioreactors were run in parallel, fed on synthetic wastewater, for a 58-day preliminary acclimation period. On day 0 (D0) the inoculum was taken from aeration tanks of the Ulu Pandan Water Reclamation Plant in Singapore, mixed well and distributed to all six reactors (2 L each). Each reactor additionally received 2 L of synthetic wastewater for a working volume of 4 L. The reactors were run under identically on nonstop 12-h cycles during the acclimation period.

The stages of each 12-h cycle were as follows: 20 min feeding, 180 min anoxic mixing, 440 min aeration and mixing (dissolved oxygen, DO, maintained at 1-2 mg/L using a feedback loop with aeration beginning at 1 L air/min when probes measured DO below 1 mg/L, and stopping when DO was above 2 mg/L), 50 min settling and 30 min effluent (supernatant) discharge. 2 L of effluent were discharged at the end of every cycle and replaced with 2 L of synthetic wastewater at the beginning of the next 12-h cycle, resulting in a hydraulic retention time of 24 h. The mixed liquor temperature was maintained at 30°C using water jackets around the reactors and a re-circulating water heater. Solids were removed regularly from mixed liquor to maintain an SRT of about 30 d.

The synthetic wastewater fed to all six reactors in the feed phase of each cycle during the acclimation period was adapted from Hesselmann *et al.* (1999) and contained (mg/L in mixed liquor in each reactor after feeding and being diluted in mixed liquor): sodium acetate (112.5), dextrose (45), yeast extract (67.5), soy peptone (60), meat peptone (60), casein peptone (90), urea (15), ammonium bicarbonate (90), ammonium chloride (169), disodium hydrogen phosphate (720), potassium dihydrogen phosphate (130), calcium chloride dihydrate (10.5) and magnesium sulphate heptahydrate (112.5). The medium also contained 2 mL of the unaltered trace element stock (Hesselmann *et al.*,1999) per liter of medium. The first six macrocomponents contributed to the COD, amounting to about 500 mg/L in the mixed liquor; the next three (ammonium-based) components contributed to the total nitrogen concentration of about 70 mg N/ L; and the phosphates were used to buffer the medium and maintain a pH around 7.5 to facilitate nitrification.

On D59, the 3-CA experiment was started and continued for about four months. At the start of this experiment, three reactors were randomly assigned to the treatment group (with 3-CA added to their feed as described below) and the other three were assigned to the control group (no 3-CA addition). The 3-CA reactors were designated T1, T2 and T3, and the control reactors were C1, C2 and C3. Cycle conditions and other parameters were identical acclimation phase conditions in all six reactors. The medium fed to the treatment reactors was slightly from that described above: the organic constituents (sodium acetate, dextrose, yeast extract, soy peptone, meat peptone and casein peptone) were scaled down by 20%, resulting in a total COD of 400 mg/L. The remaining 20% of the COD was as 3-CA, resulting in a mixed liquor 3-CA concentration of about 70 mg/L. The three control reactors continued to receive the same 3-CA-free medium used during acclimation. The 3-CA experiment lasted for 132 days, or roughly 4 SRTs. On D99, a pulse 3-CA load was inadvertently added to

control reactor C3, at the same concentration as the treatment reactors. The process impacts of this error are captured in the supplemental information, but the results from the time points shown main figures are either prior to this error, or were captured after its impacts had dissipated.

2.2 Sludge sampling for molecular analyses

To assess the changes in community composition, community function, and treatment performance over the long term, samples of sludge and effluent were taken from all six reactors at five distinct time points during the experiment; specifically, on D0 (inoculation of all six reactors), D56 (shortly before 3-CA input began), D63 (shortly after 3-CA input began), D112, D164 and D176. The last three sampling dates represent periods where 3-CA degradation had fully developed in treatment reactors. Sludge was collected directly from the mixed liquor, aliquoted into 1-mL cryogenic tubes, flash-frozen immediately in liquid nitrogen and stored at -80°C for subsequent molecular analysis. Sludge samples were also taken hourly during a single cycle study on D171 for RNA extraction and sequencing. These samples were flash-frozen and stored as described above and subjected to RNA extraction and sequencing as described in Section 2.9.

2.3 Sampling for full-cycle process performance assessment

To investigate microbial community activity and nutrient cycling across all six bioreactors, intensive sampling was carried out during 12-h cycles roughly every two weeks during the experiment. These intensive sampling regimes are henceforth called cycle studies. In all, ten cycle studies were conducted throughout the 3-CA experiment, on D59 (first day of 3-CA addition to treatment reactors), D80, D95, D110, D124, D129, D136, D158, D171 and D192. Results from only five representative cycle studies (D59, D95, D124, D158 and D192) are presented in the main figures (Figures 1 – 2), while all cycle study results are in supplemental information (Figures S1 – S5).

During a cycle study, samples were taken from all reactors at several time points. The first background sample of effluent (supernatant) was taken at the end of the settling phase, 30 min before the cycle under study commenced. Mixed liquor samples were then taken hourly during the anoxic phase, starting 30 min after the cycle started, up to the anoxic-aerobic interface. During the aerobic phase, mixed liquor was sampled every 90 min (D59 to D129) or every 30 min (D136 to D192), until the beginning of the settling phase. Then a final effluent sample was taken at the end of the settling phase. All samples were centrifuged at

8000*g* for 3 min, and the supernatant filtered through a 0.2-μm filter for nutrient analyses as described in section 2.5.

2.4 Water quality parameters

Water quality parameters were measured using standard nutrient analysis techniques per Standard Methods (APHA-AWWA-WEF, 1998), targeting COD (Standard Methods 5220 D) and nitrogen species (ammonium, nitrite and nitrate) using ion chromatography (Standard Methods 4500-NH3 for ammonium; 4110 B for nitrate and nitrite). 3-CA was measured on a Shimadzu Prominence high pressure liquid chromatography (HPLC) system (Shimadzu Corporation, Kyoto, Japan) equipped with a UV-VIS PDA detector using an Ascentis C18 5-μm column (Sigma-Aldrich, St. Louis, Missouri, USA). An isocratic 50:50 water:methanol solvent was used at a flow of 0.3 mL/min, and 3-CA peaks were identified and measured at 199, 237 and 286 nm.

2.6 DNA extraction

Genomic DNA was extracted from sludge samples from the reactors as described in Santillan *et al.* (2021).

2.6 16S rRNA gene amplicon sequencing and bioinformatics

Extracted DNA from D0, D56, D63, D112 and D164 were amplified using primer set 530f/U1053r targeting the V3~V4-V5 variable regions of the bacterial 16S rRNA gene (Thijs *et al.*, 2017). The details of the PCR reactions and subsequent purification for sequencing are as described in Santillan *et al.* (2021).The libraries were sequenced in-house at the Singapore Centre on Environmental Life Sciences Engineering (SCELSE) and sequenced sample libraries were processed as described in Santillan *et al.* (2021). Whole microbial community-level analysis of this data is available elsewhere (Santillan *et al.*, 2021).

2.7 Metagenomics sequencing and bioinformatics

Sludge from all six reactors on D176 of the experiment was used for metagenomics sequencing. Genomic DNA was extracted as described in Section 2.6 and sequenced at SCELSE on an Illumina HiSeq platform (Illumina, Inc., San Diego, California, USA). Prior to library preparation, the quality of the DNA samples was assessed on a Bioanalyzer 2100 using a DNA 12000 Chip (Agilent Technologies, Santa Clara, California, USA). Library preparation was performed by following Illumina's TruSeq DNA Nano Sample Preparation protocol, starting with 100 ng of genomic DNA and following the sizing instructions for

350bp inserts. During adapter ligation, each library was tagged with one of Illumina's TruSeq LT DNA barcodes. Library quantification was performed using Invitrogen's Picogreen assay and the average library size was determined by running the libraries on an Agilent Bioanalyzer DNA 7500 chip. Library concentrations were normalized to 4 nM and validated by qPCR on an Applied Biosystems ViiA-7 real-time thermocycler using qPCR primers recommended in Illumina's qPCR protocol, and Illumina's PhiX control library as standard. Libraries were then pooled and sequenced across two lanes of an Illumina HiSeq 2500 rapid sequencing run at a read-length of 150-bp paired-end.

In total, around 634 million paired-end reads were generated, with 105 ± 3 million paired-end reads on average per sample. Identification and quantification of functional genes was performed using the SqueezeMeta pipeline (Tamames and Puente-Sánchez, 2019). Read pairs were co-assembled using Megahit (Li *et al.*, 2015), generating 2.1 million contigs which represented 2,649 million nucleotides. Open reading frames (ORFs) were then predicted from contigs using Prodigal (Hyatt *et al.*, 2010), from which 12 million ORFs were identified, 2 ± 0.1 million ORFs on average per sample. Functional annotation was performed using DIAMOND (Buchfink *et al.*, 2015) against the KEGG database (Kanehisa *et al.*, 2016). Read mapping against contigs was then performed using Bowtie2 (Langmead and Salzberg, 2012) in order to quantify the abundance of genes among the different samples, and transformed to transcripts per million (TPM) values (Puente-Sánchez *et al.*, 2020). To identify genes involved in 3-CA degradation, the analysis focused on the following KEGG metabolic pathways from the xenobiotics biodegradation and metabolism category: chlorocyclohexane and chlorobenzene degradation (KO: 00361), benzoate degradation (KO: 00362), polycyclic aromatic hydrocarbon degradation (KO: 00624), and aminobenzoate degradation (KO: 00627). A total of 170 genes were recovered from these pathways.

2.8 RNA extraction, sequencing and transcriptomics

Methods for total RNA extraction have been described in Law et al (2016). RNA extractions were performed with Soil/ Fecal RNA Isolation Kit (Zymo Research, Irvine, CA, USA; Catalog# R2040) with some protocol modifications (Law et al, 2016). RNA purity was determined by Thermo Scientific Nanodrop 2000 by calculating an A260/A280 and A260/A230 to screen for contaminants in purified RNA. Extracted RNA concentration was determined by a Qubit 2.0 fluorometer, and RNA integrity (RIN) was measured using the Agilent 2200 Tapestation system, prior to library preparation and sequencing on an Illumina 2500 using a 101 bp paired-end run (Law et al, 2016). Reads of non-ribosomal origin were

mapped to predicted genes in the metagenome assembly, converted to reads per kilobase million (rpkm) and aggregated using the same annotations used above.

2.9 Data Analysis

2.9.1 Nitrifier Abundance Analysis

To examine relative nitrifier abundance via 16S rRNA amplicon sequencing, all ASVs identified as AOB or NOB were extracted, with their normalized read counts. Relative abundances were calculated compared to the total read count of all ASVs in each sample. The change in AOB and NOB relative abundances were then calculated over time and across control and treatment reactors, as individual ASVs as total AOB or NOB.

2.9.2 Identification of ASVs associated with 3-CA Degradation

To determine which ASVs from 16S rRNA amplicon sequencing were correlated with 3-CA degradation in treatment reactors, each ASV from each treatment reactor from D64, D112 and D164 was compared to 3-CA degradation rates in each treatment reactor on D59, D110 and D171, respectively. The comparisons were not possible on the same days because 3-CA degradation data were not taken on the same days where sludge samples were taken for amplicon sequencing. However, the variation in 3-CA degradation did not differ widely over time once 3-CA degradation had been established, so these comparisons were still considered valid. Spearman's rank order correlation coefficient was used between the three 3-CA removal percentages on the three days identified above, and the corresponding normalized ASV abundances in the three treatment reactors ($n = 9$: 3 time points × 3 reactors). To assess correlation significance, T-statistics were calculated from the correlation coefficient for each ASV based on 7 ($n - 2$) degrees of freedom, and p-values were calculated from these T-statistics. A 10% False Discovery Rate (FDR) correction was then applied to adjust for multiple comparisons.

The mean normalized abundance of each taxon across all three treatment reactors on D63, D112 and D164 was plotted on a logarithmic scale against the respective 3-CA degradation correlation coefficient as calculated above (Figure 5). ASVs that fell toward the top right of this plot and correlated with relevant degradation genes as identified below were considered more likely to have participated in 3-CA degradation.

2.9.3 Differential enrichment of xenobiotics degradation genes

To determine which xenobiotics degradation genes from the metagenomics data set from D176 were differentially enriched, the tpm values for each gene in all six reactors were

used. A z-score was first calculated for each gene in each reactor, to determine the deviation from the average tpm. The difference in mean z-score between control and treatment reactors was then calculated, termed D_z. Differential enrichment in treatment reactors was defined as $D_z \geq 1.4$. This cutoff was chosen to balance selection of genes enriched by 3-CA presence and degradation, given the small sample size and the false elimination of genes likely to have degraded 3-CA (*i.e.*, reducing type II error probability). Thus, out of the initial 170 genes, 32 were flagged as differentially enriched (Table S1). Subsequently, to assess significance of enrichment, two-tailed Welch's t-tests were performed on the 32 flagged genes, adjusting corresponding p-values for multiple comparisons under a 10% FDR. Eight genes were identified as significantly enriched in treatment reactors. The 32 genes that were differentially enriched ($D_z \geq 1.4$) and the eight that were significantly differentially enriched ($D_z \geq 1.4$ and p-value < 0.1 after 10% FDR correction) are identified in Table S1. Of the 32 genes identified in Table S1, seven that were additionally assumed to have played a role in 3-CA degradation were identified in Table 1 and are discussed further.

2.9.4 Differential transcription of xenobiotics degradation genes from metatranscriptomics data

To determine whether the differentially enriched genes were also differentially transcribed in response to 3-CA input, we checked whether the transcription levels of a given gene related to 3-CA degradation rose during the aerobic phase of a cycle in treatment reactors compared to control reactors, and compared to the anoxic phase. The rpkm values for each relevant gene during a full cycle on D171 were plotted, including local polynomial regression fitting using the *loess* function from the *ggplot2* package (v.3.3.2) in R, including 95% confidence intervals.

3 Results and discussion

We investigated the effects of a sustained disturbance, caused by the presence of the xenobiotic compound 3-CA on nitrification and the nitrifying microbial community. Additionally, the advent of 3-CA degradation led to the identification of putative 3-CA degraders and their associated degradation pathways.

3.1 Impact of 3-CA on community function

Nutrient profiles from all six reactors over several 12-h cycle studies revealed the impact of sustained 3-CA input on community function (Figures 1, 2 and S1 – S5). In the anoxic phase, control reactors consistently showed degradation of COD (Figure 1B, S2B) and

nitrate (Figure 2C, S5B), with a transient nitrite spike (Figure 2B, S4B), indicating a complete denitrification pathway. The control reactors also showed complete nitrification in the aerobic phase, with ammonia levels falling < 5 mg/L (Figure 2A, S3B) (apart from D110, where an inadvertent 3-CA input into reactor C3 caused temporary ammonia oxidation loss), an accompanying nitrite spike (Figure 2B, S4B) and subsequent nitrate build-up (Figure 2C, S5B). On the other hand, the treatment reactors initially saw partial COD degradation in the anoxic phase, which began to improve over time, as indicated by the progression of COD profiles from D59 to D192, with COD levels on D124 comparable to those of the control reactors (Welch's t-test P = 0.6) at the end of the cycle (Figure 1B, S2A). Ammonia oxidation was inhibited in treatment reactors in the aerobic phase (Figure 2A, S3A), with ammonia accrual seen over multiple consecutive cycles. However, some ammonia oxidation was seen in treatment reactors starting on D158 (Figure 2A, S3A), accompanied by some nitrite production in the aerobic phase (Figure 2B, S4A). These results indicated that COD reduction, followed by ammonia oxidation, gradually began to recover in treatment reactors, despite the continuing 3-CA input.

Concurrent with the COD degradation that developed starting on D95 in the treatment reactors at the beginning of the aerobic phase (Figure 1B, S2A), 3-CA degradation started to occur consistently in all three treatment reactors (Figure 1A, S1), indicating that 3-CA accounted for the portion of COD degraded in the treatment reactors during the aerobic phase. 3-CA degradation was evident from the onset of aeration from D95 onwards, implying that the treatment reactors had developed the ability to degrade 3-CA in response to sustained input. In turn, other processes like ammonia oxidation started to recover despite continued 3-CA input, as indicated above.

Separate batch experiments were performed on the sludge from all six reactors to confirm that 3-CA degradation was occurring biologically. These batch experiments are described in the Supplemental Information, and the results shown in Figure S6.

The partial recovery of ammonia oxidation took about 35 days from the start of 3-CA input. Falk and Wuertz (2010) saw neither 3-CA degradation nor ammonia oxidation recovery over a 70-day experiment in replicate bench-scale reactors subjected to similar levels of sustained 3-CA input. However, their experiment was performed at a lower mixed liquor temperature (20º C versus 30º C in our experiment) and used an inoculum from a wastewater treatment plant in a different geographic region (temperate Davis, California; versus tropical Singapore) from a different sewershed (university campus, including multiple research facilities versus a residential-industrial mix in Singapore). These differences could

have led to the emergence of 3-CA degradation and nitrification recovery in our reactors versus theirs. Santillan *et al.* (2019b) reported 3-CA degradation, but no nitrification recovery, in a 35-day replicated experiment that included sustained 3-CA input, and partial ammonia oxidation recovery with less frequent 3-CA pulses.. While their inoculum was from the same plant as ours, they used a much smaller reactor volume, about 20 mL. Ma *et al.* (2020) reported full nitrification recovery within about 12 days of a pulse 3-CA input (at lower concentrations), in a single-reactor study, possibly concurrent with the washout of 3-CA from the reactor. Kelly *et al.* (2004) reported a 17-day recovery period for total nitrification for a pulse 1-chloro-2,4-dinitrobenzene shock at a comparable concentration (absolute, and relative to total COD) in a pilot-scale reactor. The partial nitrification our study may be attributed to the long SRT of 30 days. This allowed AOB to acclimate to the sustained 3-CA input. The onset of 3-CA degradation likely helped this AOB recovery process. To summarize, the present study saw 3-CA degradation develop, followed by the recovery of ammonia oxidation. Both processes were likely aided by the source inoculum and the long SRT.

3.2 Changes in the nitrifier community

Nitrifier community dynamics were assessed in control and treatment reactors in terms of total nitrifiers (Figure 3A), AOB (Figure 3B) and NOB (Figure 3C). During the acclimation period there was little change in the mean relative abundances of nitrifiers, AOB or NOB, because all six reactors were treated identically. With the start of 3-CA input into the three treatment reactors on D59, the total nitrifier relative abundance dropped initially in all six reactors, and then rose over time in the control reactors, with little change over time for the treatment reactors. Reactor C3, which received an accidental 3-CA pulse input on D99, showed similar total nitrifier numbers as the treatment reactors on D112. In terms of AOB community, there were no differences between treatment and control reactors during the experiment, with a steady rise in mean abundance in all reactors. Total NOB numbers dropped in treatment reactors after 3-CA input, as well as in C3 on D112, while numbers in control reactors generally rose. Figure 4 shows relative abundances of nitrifiers in control (Figure 4A), treatment (Figure 4B) and all (Figure 4C) reactors and partitioned by ASV. While the loss of NOB in the treatment reactors is demonstrated clearly, AOB recovery is also seen, with a modified AOB community. This indicates that NOB were more affected by 3-CA input than AOB and did not recover in treatment reactors.

AOB and NOB ASVs were primarily represented by the genera *Nitrosomonas* (two out of five AOB ASVs identified) and *Nitrospira* (two out of three NOB ASVs identified), respectively. Unassigned-species *Nitrosomonas* reads dominated in the control reactors, while the treatment reactors saw an increase in *Nitrosomonadacaea Ellin6067* and *Nitrosomonas europaea*.

It should be noted that the amplicon sequencing data do not imply absolute abundances of any taxon. They do, however, represent abundances relative to the total community sampled by the 16S rRNA gene amplicon used (Sanapareddy *et al.*, 2009, Poretsky *et al.*, 2014). Nitrification loss with 3-CA input, was likely because of 3-CA directly impacting the AOB community. In addition to its general biotoxicity (Boon *et al.*, 2003; Shah 2014), 3-CA acts as a suicide substrate for the ammonium monooxygenase enzyme, which normally initiates the ammonia oxidation process (Reineke, 1998). The resulting loss of ammonia oxidation likely cascaded into the loss of nitrite oxidation, and the subsequent fall in both AOB and NOB in the treatment reactors. AOB likely recovered after the onset of 3-CA degradation, once the enzyme was no longer blocked from executing its regular function in the aerobic phase.

NOB recovery was not seen in the treatment reactors for two possible reasons. The first reason is that, with only partial ammonia oxidation recovery during the experiment, there was inadequate nitrite production to induce NOB regrowth. Conversely, it is also conceivable that nitrite oxidation never resumed because NOB did not regrow. The second possible reason is that NOB were more severely impacted by 3-CA toxicity. AOB are more resilient to toxic compounds than NOB because they can undergo oxidative stress and up-regulate maintenance enzymes (Geets *et al.*, 2006; Ge *et al.*, 2015; Laloo *et al.*, 2018). Indeed, the inability of NOB to recover from sustained toxin input has been documented (mostly in unreplicated studies), with respect to 4-CA (Zhu *et al.*, 2014), phenol (Alves *et al.*, 2017) and triclocarban (Bian *et al.*, 2020).

Overall AOB relative abundances were maintained in treatment reactors throughout the experiment, but the internal AOB community structure shifted (Figure 4). On D112 and D164, well into stable 3-CA degradation, the AOB communities in treatment reactors were dominated by *Nitrosomondaceae Ellin6067* and *N. europaea*. This contrasts with treatment reactors prior to D112, and to control reactors at any time. *N. europaea* is a model AOB, sometimes found in nitrifying activated sludge (Perez-Garcia *et al.*, 2014). It is also involved in aromatics degradation (Keener and Arp, 1994; Sun *et al.*, 2019), and its xenobiotics tolerance relative to other AOBs may have contributed to its maintenance and relative

emergence in treatment reactors. While researchers have found overall reduction in AOB relative abundance with the input of a toxic chemical (Zhu *et al.*, 2014; Wu *et al.*, 2016; Luan *et al.*, 2020), the dynamics of AOB community composition due to a sustained toxin input in a controlled and replicated experiment have not been demonstrated before.

3.3 Organisms and pathways involved in 3-CA degradation

The emergence of 3-CA degradation in the treatment reactors led to a search for the degrading organisms and their likely degradation pathways. Enrichment and isolation of 3-CA-degrading organisms using cultivation methods were unsuccessful (data not shown). We therefore turned to the molecular data collected – taxonomic data from amplicon sequencing, functional gene enrichment data from assembled metagenomics, and gene transcription data from metatranscriptomics – to evaluate potential 3-CA degraders and relevant functional genes.

3.3.1 Organisms associated with 3-CA degradation

While the identities of the actual 3-CA degrading organisms could not be established with our data, we identified three genera that significantly correlated with degradation in all three treatment reactors after FDR correction, namely *Gemmatimonas*, *OLB8* and *Taibaiella* (Figure 5).

While *Gemmatimonas* has generally been found in a diverse range of activated sludge systems (Zhang *et al.*, 2012; Ju *et al.* 2014), Santillan *et al.* (2019) additionally found this genus enriched under sustained 3-CA input conditions similar to ours. *OLB8* has not been associated with aromatics degradation before to our knowledge, but it belongs to the family *Saprospiraceae*, which is found in high-stress environments like low-temperature nitrifying sludge (Johnston *et al.*, 2019) and has been associated with antibiotics resistance (Luan *et al.*, 2020). Commonly found in activated sludge as a hydrolyser, it is thought to provide for the breakdown of complex organics (McIlroy and Nielsen, 2014; Szabo *et al.*, 2017). However, the family has not been directly associated with the degradation of aromatic compounds. The third genus we identified, *Taibaiella*, has been found in phenol-degrading microbial communities in microbial fuel cells (Shen *et al.*, 2020), in petroleum-contaminated soil (Diallo *et al.*, 2021) and in toxic landfill leachate (El-Fadel *et al.*, 2018), indicating tolerance to xenobiotics, if not an ability to degrade them. *Gemmatimonas*, *OLB8*, and *Taibaiella* were significantly correlated with 3-CA degradation not only due to their stress tolerance, but may also have been responsible for its degradation. Other ASVs that correlated (but not

significantly) with 3-CA degradation included *Dokdonella*, *Burkholderia ottowia*, and two species of the genus *Sphingobacteriales*. Sun *et al.* (2019) found *Sphingobacteriales* associated with aromatics degradation genes in phenol-degrading activated sludge bioreactors. Other *Burkholderia* species have also been found to degrade aromatics like phenol (Ma *et al.*, 2020b), and *Dokdonella* has been associated with the degradation of paracetamol (Palma *et al.*, 2018) and polycyclic aromatic hydrocarbons (Bacosa and Inoue, 2015).

3.3.2 Differential enrichment of putative 3-CA degrading genes

3-CA is usually degraded by oxidation to a chlorocatechol (upper pathway) by oxidative deamination, followed by ring cleavage and subsequent degradation into tricarboxylic (TCA) cycle intermediates (lower pathway) (Reineke, 1998; Bathe, 2004; Fuchs *et al.*, 2011). Therefore, we aimed to identify the upper pathway via searching for a mono- or dioxygenase, and the lower pathway via a ring cleavage enzyme.

Using assembled metagenomics data from D176, multiple upper and lower pathway genes were identified via the KEGG database (Aoki and Kanehisa, 2012), of which several were differentially enriched in the treatment reactors (Table S1). The enzyme involved in the first 3-CA oxidation step would theoretically be chloroaniline dioxygenase (Krol *et al.*, 2012); unfortunately, its presence could not be validated because of the lack of a KEGG ortholog for the gene encoding it. Also, chloroaniline dioxygenase may not have been present in the inoculum because it has a narrow substrate specificity (Krol *et al.*, 2012) and may therefore not be commonly present in activated sludge metagenomes. Other upper pathway genes were identified as putative contributors to 3-CA degradation, based on their ability to oxidize aromatic compounds and their differential enrichment in the treatment reactors (Table 1, Table S1). These include benzoate/toluate 1,2-dioxygenase, benzene/toluene dioxygenase, 2,4-dichlorophenol 6-monooxygenase and phenol/toluene 2-monooxygenase. All of them were enriched in treatment reactors ($D_z \geq 1.4$), but the last two were not significantly enriched after FDR correction. They all normally act on their respective eponymous substrates. It is unclear whether chlorophenol enzymes can be induced by chloroaniline. However, toluene dioxygenase has been shown to degrade chloroanilines, including 3-CA (Nitisakulkan *et al.*, 2014), and benzoate dioxygenase has been associated with aniline degradation (Zhang *et al.*, 2021). Furthermore, toluene dioxygenase has a broader substrate specificity and can be induced by chloroanilines (Semak *et al.*, 2012). Thus, all these enzymes were considered potential candidates for initiating 3-CA degradation.

In terms of the potential lower degradation pathway for 3-CA, we focused on the relevant ring cleavage enzyme, because genes involved in subsequent segments of the lower pathway are relatively common. The two major ring cleavage pathways for most chlorinated aromatics involve an ortho-cleavage or a meta-cleavage enzyme (Reineke, 1998). One enzyme of each type was enriched in the treatment reactors ($D_z \geq 1.4$) – a catechol 2,3-dioxygenase (associated with meta-cleavage, potentially via 4-chlorocatechol) and a chlorocatechol 1,2-dioxygenase (associated with ortho-cleavage, via 3- or 4-chlorocatechol) (Table 1, Table S1). However, neither of these enzymes was significantly differentially enriched. Additionally, the meta-cleavage enzyme was a catechol dioxygenase, not a chlorocatechol dioxygenase, and there is some evidence that catechol dioxygenases may not be induced by their chlorinated counterparts (Radianintyas *et al.*, 2003). Therefore, it is more likely that the lower degradation pathway involved an ortho-cleavage pathway via the chlorocatechol 1,2-dioxygenase.

3.3.3 Differential transcription of putative 3-CA degrading genes

Transcriptomics data from all six reactors on D171 were used to determine whether the upper and lower pathway genes identified above were transcribed in real time during a reactor cycle. Genes that were likely contenders for 3-CA degradation would be transcribed at higher levels in treatment reactors during the aerobic phase (when 3-CA removal occurred).

Four upper pathway genes were identified as likely contenders in Section 3.3.2. Of these, the mean transcription levels of 2,4-dichlorophenol 6-monooxygenase (K10676; *tfdB*) were elevated in treatment reactors during the aerobic phase (Figure 6D). Of the two lower pathway genes identified earlier, chlorocatechol 1,2-dioxygenase (K15253; *tfdC*) also showed differential transcription in the treatment reactors during the aerobic phase (Figure 6B). Even though these genes were not significantly differentially enriched (Table 1), their clear differential transcription makes them more likely contenders for 3-CA degradation. The transcription levels of other major enzymes identified via metagenomics data as potential participants in 3-CA degradation were not as clearly higher in treatment reactors during the aerobic phase. While the likely intermediate, 4-chlorocatechol, was not measured in this experiment, the differential transcription of *tfdB* and *tfdC* in Figures 6D and 6B respectively indicates the formation of a complete pathway – the upper pathway, encoded by *tfdB* or 2,4-dichlorophenol 6-monooxygenase (K10676) showing differential transcription with the onset of aeration; and the lower pathway encoded by *tfdC* or chlorocatechol 1,2-dioxygenase

(K15253) differentially transcribed toward the second half of the aerobic phase, likely with the build-up of the intermediate compound.

Gu *et al.* (2017) found both ortho- and meta-cleavage genes simultaneously transcribed in *Acinetobacter* pure cultures degrading phenol. Similarly, Sun *et al.* (2019) demonstrated differential transcription of phenol degrading genes in nitrifying activated sludge batch cultures via an ortho-cleavage pathway. Sato *et al.* (2019) also found differential enrichment and transcription of several aromatics degradation genes in response to heavy oil inputs to duplicate activated sludge reactors. However, all these studies used long-term sampling for gene transcription. Given the short half-life of mRNA (Selinger *et al.*, 2003), RNA profiles in a complex community like activated sludge can change rapidly. This study is the first to our knowledge to consistently show the rise and fall in the transcription of genes related to a potential degradation pathway in the short term, within a single cycle phase.

When combined with the finding of differential enrichment of several aromatics degradation genes and the process data showing 3-CA degradation in replicate reactors, the differential transcription data make it likely that 3-CA degradation occurred via a modified ortho-cleavage pathway via a dichlorophenol monooxygenase and a chlorocatechol dioxygenase.

4 Conclusions

In this study, we ran a controlled experiment to investigate the impact of sustained 3-chloroaniline input on replicated wastewater-treating bioreactors from a process and microbial community perspective.

- Full removal of 3-CA was observed in all three treatment reactors with time (after a three-week period of sustained input) with the recovery of ammonia oxidation.
- Major differences were found in nitrifier community succession in treatment reactors. The AOB community recovered with the onset of 3-CA degradation, albeit after a major shift in its internal structure compared to that of the control reactors. The nitrite-oxidizing community did not recover from the 3-CA input.
- Using a combination of metagenomics and metatransciptomics, a putative pathway for 3-CA degradation was identified via a phenol monooxygenase and a subsequent ortho-cleavage enzyme.
- Several taxa correlated significantly with 3-CA degradation, including *Gemmatimonas*, *Saprospiraceae OLB8* and *Taibaiella*. It is possible that multiple taxa were responsible for 3-CA degradation via patchwork pathway assembly.

Acknowledgements

This work was funded by the Singapore Ministry of Education and the National Research Foundation under an RCE grant awarded to the Singapore Centre for Environmental Life Sciences Engineering (SCELSE). The authors would like to thank Ms Angel Anisa Cokro (SCELSE) and Ms Angel Anika Cokro (SCELSE), Ms Anita Ng (Singapore Polytechnic) and Mr Sean Chew (Singapore Polytechnic) for their help with reactor operation and sample processing; Mr Larry Liew Chee Wai (SCELSE) for his help with sludge collection and storage; Dr Daniela Drautz-Moses and colleagues from the SCESLE sequencing core facility for obtaining short read sequencing data used in this study; Krithika Arumugam for data processing and bioinformatics and Dr Siao Yun Chang (PUB Technology) and her colleagues from PUB Water Reclamation (Plants) for providing us access to the Ulu Pandan Water Reclamation Plant for sludge collection.

Author Contributions

SW and HS conceived the study and SW obtained the funding. HS designed the study and performed the experiments. HS and ES performed the molecular work to prepare samples for 16S rRNA gene amplicon and metagenomics sequencing, while USCS did it for metatranscriptomics sequencing. ES did the bioinformatic analysis on the 16S rRNA gene amplicon sequences; FC performed metagenomics assembly bioinformatics; and RW analyzed the transcriptomics data. HS and ES interpreted individual data sets; HS elaborated the main arguments in the manuscript; other authors contributed to individual sections and edited the draft.

Data Availability

DNA sequencing data are available at NCBI BioProjects under accession numbers PRJNA720804 and PRJNA720805. See supplemental information for details about the 3-CA degradation batch experiment, the calculation of 3-CA degradation rates in treatment reactors, a list of genes associated with xenobiotics degradation that were differentially enriched in treatment reactors, and chemical profiles over single 12-h cycles for all reactors measured at ten different days of the study.

Competing Interests

The authors declare no competing interests.

References

Albertsen, M., *et al.* (2012). A metagenome of a full-scale microbial community carrying out enhanced biological phosphorus removal. ISME Journal **6**(6): 1094-1106.

Alves, A. P. A., *et al.* (2017). Impact of phenol shock loads on the performance of a combined activated sludge-moving bed biofilm reactor system. International Biodeterioration & Biodegradation, 123, 146-155.

Aoki, K. F., & Kanehisa, M. (2005). Using the KEGG database resource. Current Protocols in Bioinformatics, 11(1), 1-12.

APHA-AWWA-WEF (1998). Standard Methods for the Examination of Water and Wastewater.

Buchfink, B., *et al.* (2015). Fast and sensitive protein alignment using DIAMOND. Nature Methods, 12(1), 59-60.

Bacosa, H. P., and Inoue, C. (2015). Polycyclic aromatic hydrocarbons (PAHs) biodegradation potential and diversity of microbial consortia enriched from tsunami sediments in Miyagi, Japan. Journal of Hazardous Materials, 283, 689-697.

Bathe, S. (2004). Conjugal transfer of plasmid pNB2 to activated sludge bacteria leads to 3-chloroaniline degradation in enrichment cultures. Letters in Applied Microbiology **38**(6): 527-531.

Bian, Y., *et al.* (2020). The fate and impact of TCC in nitrifying cultures. Water Research, 115851.

Boon, N., *et al.* (2000). Bioaugmentation of activated sludge by an indigenous 3-chloroaniline-degrading Comamonas testosteroni strain, I2gfp. Applied and Environmental Microbiology **66**(7): 2906-2913.

Boon, N., *et al.* (2003). Bioaugmentation as a tool to protect the structure and function of an activated-sludge microbial community against a 3-chloroaniline shock load. Applied and Environmental Microbiology **69**(3): 1511-1520.

Briones, A. and L. Raskin (2003). Diversity and dynamics of microbial communities in engineered environments and their implications for process stability. Current Opinion in Biotechnology **14**(3): 270-276.

Buchfink, B., *et al.* (2015). Fast and sensitive protein alignment using DIAMOND. Nature Methods 12(1), 59-60.

Callahan, B.J., *et al.* (2016). DADA2: High resolution sample inference from Illumina amplicon data. Nature Methods 13(7), 581-583.

Callahan, B.J., *et al.* (2017). Exact sequence variants should replace operational taxonomic units in marker-gene data analysis. ISME Journal 11, 2639–2643.

Cauduro, G.P., *et al.* (2020). Differential Expression and PAH Degradation: What Burkholderia vietnamiensis G4 Can Tell Us? International Journal of Microbiology, Article ID 8831331.

Chen, C., *et al.* (2014). Software for pre-processing Illumina next-generation sequencing short read sequences. Source Code for Biology and Medicine 9, 8-8.

Cui, J., *et al.* (2020). Comparison of bacterial community structure and function under different petroleum hydrocarbon degradation conditions. Bioprocess and Biosystems Engineering, 43(2), 303-313.

Delatolla, Robert, *et al.* (2012). Effects of long exposure to low temperatures on nitrifying biofilm and biomass in wastewater treatment. Water Environment Research 84.4: 328-338.

Diallo, M. M., *et al.* (2021). Enhanced biodegradation of crude oil in soil by a developed bacterial consortium and indigenous plant growth promoting bacteria. Journal of Applied Microbiology 130(4), 1192-1207.

El-Fadel, M., *et al.* (2018)."Impact of SRT on the performance of MBRs for the treatment of high strength landfill leachate. Waste Management, 73, 165-180.

Falk, M. W. and S. Wuertz (2010). Effects of the toxin 3-chloroaniline at low concentrations on microbial community dynamics and membrane bioreactor performance. Water Research **44**(17): 5109-5115.

Ficara, E. and A. Rozzi (2001). pH-stat titration to assess nitrification inhibition. Journal of Environmental Engineering-ASCE **127**(8): 698-704.

Fuchs, G., *et al.* (2011). Microbial degradation of aromatic compounds—from one strategy to four. Nature Reviews Microbiology, 9(11), 803-816.

Ge, S., *et al.* (2015). Detection of nitrifiers and evaluation of partial nitrification for wastewater treatment: A review. Chemosphere, 140, 85-98.

Geets, J., *et al.* (2006). Strategies of aerobic ammonia-oxidizing bacteria for coping with nutrient and oxygen fluctuations. FEMS microbiology ecology, 58(1), 1-13.

Glöckner, F.O., *et al.* (2017). 25 years of serving the community with ribosomal RNA gene reference databases and tools. Journal of Biotechnology 261, 169-176.

Henriques, I. D., *et al.* (2007). Activated sludge inhibition by chemical stressors—a comprehensive study. Water Environment Research, 79(9), 940-951.

Hesselmann, R. P. X., *et al.* (1999). Enrichment, phylogenetic analysis and detection of a bacterium that performs enhanced biological phosphate removal in activated sludge. Systematic and Applied Microbiology **22**(3): 454-465.

Huson, D. H. and N. Weber (2013). Microbial Community Analysis Using MEGAN. Microbial Metagenomics, Metatranscriptomics, and Metaproteomics. E. F. DeLong. San Diego, Elsevier Academic Press Inc. **531:** 465-485.

Hwang, C., *et al.* (2006). Changes in bacterial community structure correlate with initial operating conditions of a field-scale denitrifying fluidized bed reactor. Applied Microbiology and Biotechnology **71**(5): 748-760.

Hyatt, D., Chen, *et al.* (2010). Prodigal: prokaryotic gene recognition and translation initiation site identification. BMC Bioinformatics 11(1), 119.

Johnston, J., *et al.* (2019). Composition and dynamics of the activated sludge microbiome during seasonal nitrification failure. Scientific Reports, 9(1), 1-15.

Ju, F., et al (2014). Taxonomic relatedness shapes bacterial assembly in activated sludge of globally distributed wastewater treatment plants. Environmental Microbiology 16(8), 2421-2432.

Ju, F., and Zhang, T. (2015). Bacterial assembly and temporal dynamics in activated sludge of a full-scale municipal wastewater treatment plant. The ISME journal, 9(3), 683-695.

Kanehisa, M., *et al.* (2016). KEGG as a reference resource for gene and protein annotation. Nucleic Acids Research 44(Database issue), D457-D462.

Keener, W. K. and D. J. Arp (1994). Transformations of Aromatic Compounds by Nitrosomonas Europaea. Applied and Environmental Microbiology **60**(6): 1914-1920.*

Kelly, R. T. *et al.* (2004). Chemical Inactivation of Nitrification in Activated Sludge. Biotechnology and bioengineering, 85(6), 683-694.

Krol, J. E., *et al.* (2012). Role of IncP-1 beta Plasmids pWDL7::rfp and pNB8c in Chloroaniline Catabolism as Determined by Genomic and Functional Analyses. Applied and Environmental Microbiology **78**(3): 828-838.

Kuypers, M. M., *et al.* (2018). The microbial nitrogen-cycling network. Nature Reviews Microbiology, 16(5), 263.

Laloo, A. E., *et al.* (2018). Mechanisms of persistence of the ammonia-oxidizing bacteria Nitrosomonas to the biocide free nitrous acid. Environmental science & technology, 52(9), 5386-5397.

Langmead, B., *et al.* (2012). Fast gapped-read alignment with Bowtie 2. Nature Methods 9(4), 357-359.

Law, Y., et al (2016). Integrative microbial community analysis reveals full-scale enhanced biological phosphorus removal under tropical conditions. Scientific Reports, 6(1), 1-15.

Li, D., *et al.* (2015). MEGAHIT: an ultra-fast single-node solution for large and complex metagenomics assembly via succinct de Bruijn graph. Bioinformatics 31(10), 1674-1676.

Liu, Y. J., *et al.* (2018). Energy self-sufficient biological municipal wastewater reclamation: present status, challenges and solutions forward. Bioresource Technology, 269, 513-519.

Luan, X., *et al.* (2020). Microbial community functional structure in an aerobic biofilm reactor: Impact of streptomycin and recovery. Chemosphere, 127032.

Ma, B., Zhao, *et al.* (2020). Effects of transient 3-chloroaniline shock loading on the performance, microbial community and enzymatic activity of sequencing batch reactor. Journal of Environmental Management, 258, 110017.

Ma, Y *et al.* (2020b). Time-course transcriptome analysis reveals the mechanisms of Burkholderia sp. adaptation to high phenol concentrations. Applied Microbiology and Biotechnology, 104, 5873-5887.

McCarty, G. W. (1999). Modes of action of nitrification inhibitors. Biology and Fertility of Soils **29**(1): 1-9.

McCarty, P. L., *et al.* (2011). Domestic wastewater treatment as a net energy producer–can this be achieved? Environmental Science and Technology 45: 7100-7106.

McIlroy, S. J., and Nielsen, P. H. (2014). The Family *Saprospiraceae*. In *The prokaryotes: Other major lineages of bacteria and the Archaea*, pp. 863-889. Springer Science+ Business Media, 2014.

Nitisakulkan, T. *et al.* (2014). Degradation of chloroanilines by toluene dioxygenase from *Pseudomonas putida* T57. Journal of Bioscience and Bioengineering 117(3): 292-297.

Omelchenko MV, *et al.* (2010). Non-homologous isofunctional enzymes: a systematic analysis of alternative solutions in enzyme evolution" Biology Direct 5 (1): 31

Palma, T. L., *et al.* (2018). Putative role of Flavobacterium, Dokdonella and Methylophilus strains in paracetamol biodegradation. Water, Air, & Soil Pollution, 229(6), 1-23.

Perez-Garcia, O., *et al.* (2014). Clarifying the regulation of NO/N_2O production in *Nitrosomonas europaea* during anoxic–oxic transition via flux balance analysis of a metabolic network model. Water Research, 60, 267-277.

Pimviriyakul, P., *et al.* (2019). Microbial degradation of halogenated aromatics: molecular mechanisms and enzymatic reactions. Microbial Biotechnology, 13(1), 67-86.

Poretsky, R., *et al.* (2014). Strengths and limitations of 16S rRNA gene amplicon sequencing in revealing temporal microbial community dynamics. PloS One, 9(4), e93827.

Puente-Sánchez, F., *et al.* (2020). SQMtools: automated processing and visual analysis of ’omics data with R and anvi’o. BMC Bioinformatics 21(1), 358.

Radianingtyas, H., *et al.* (2003). Characterization of a soil-derived consortium degrading 4-Chloraniline. Microbiology, 149, 3279-3287.

Sanapareddy, N., *et al.* (2009). Molecular Diversity of a North Carolina Wastewater Treatment Plant as Revealed by Pyrosequencing. Applied and Environmental Microbiology **75**(6): 1688-1696.

Santillan, E. *et al.* (2019). Trait based life history strategies explain succession scenario for complex bacterial communities under varying disturbance. Environmental Microbiology 21.10 3751-3764.

Santillan *et al.* (2019b). Frequency of disturbance alters diversity, function, and underlying assembly mechanisms of complex bacterial communities. Npj Biofilms and Microbiomes, 5(1): 1-9.

Santillan, E., *et al.* (2020). Press disturbance alters community structure and assembly mechanisms of bacterial taxa and functional genes in mesocosm-scale bioreactors. mSystems, 5 (4): e00471-00420.

Santillan, E., *et al.* (2020b). Sustained organic loading disturbance favors nitrite accumulation in bioreactors with variable resistance, recovery and resilience of nitrification and nitrifiers. Scientific Reports, 10 (1).

Santillan, E., *et al.* (2021). Press xenobiotic 3-chloroaniline disturbance favors deterministic assembly with a shift in function and structure of bacterial communities. ACS ES&T Water (in press). DOI: 10.1021.acsestwater.1c00018.

Sato, Y., *et al.* (2019). Transcriptome analysis of activated sludge microbiomes reveals an unexpected role of minority nitrifiers in carbon metabolism. Communications Biology, 2, 1-8.

Selinger, D.W., *et al.* (2003). Global RNA half-life analysis in *Escherichia coli* reveals positional patterns of transcript degradation. Genome Research, 13, 216–223.

Semak, V. *et al.* (2012). Toluene dioxygenase mediated oxidation of halogen-substituted benzoate esters. Organic and Biomolecular Chemistry 10(22): 4407-4416.

Shah, M. P. (2014). Microbial degradation of 3-chloroanilne by two bacterial strains isolated from common effluent treatment plant. Journal of Applied Environmental Microbiology, 2, 155-165.

Shen, J., *et al.* (2020). Effect of lignite activated coke packing on power generation and phenol degradation in microbial fuel cell treating high strength phenolic wastewater. Chemical Engineering Journal, 128091.

Siripong, S. and B. E. Rittmann (2007). Diversity study of nitrifying bacteria in full-scale municipal wastewater treatment plants. Water Research **41**(5): 1110-1120.

Sun, H., *et al.* (2019). Diverse aromatic-degrading bacteria present in a highly enriched autotrophic nitrifying sludge. Science of the Total Environment, 666, 245-251.

Szabó, E., *et al.* (2017). Microbial population dynamics and ecosystem functions of anoxic/aerobic granular sludge in sequencing batch reactors operated at different organic loading rates. Frontiers in Microbiology, 8: 770.

Tam, L. T., *et al.* (2006). Differential gene expression in response to phenol and catechol reveals different metabolic activities for the degradation of aromatic compounds in *Bacillus subtilis*. Environmental Microbiology, 8(8), 1408-1427.

Tamames, J., *et al.* (2019). SqueezeMeta, A Highly Portable, Fully Automatic Metagenomic Analysis Pipeline. Frontiers in Microbiology 9(3349).

Thijs, S., *et al.* (2017). Comparative evaluation of four bacteria-specific primer pairs for 16S rRNA gene surveys. Frontiers in Microbiology 8, 1-15.

Thompson, K., Chirstofferson, W., Robinette, D., Curl, J., Baker, L., Brereton, J., and K. Reich (2006). Characterizing and Managing Salinity Loading in Reclaimed Water Systems. American Water Works Association (AWWA), USA.

Valipour, A., *et al.* (2014). Performance of high-rate constructed phytoremediation process with attached growth for domestic wastewater treatment: Effect of high TDS and Cu. Journal of Environmental Management **145**: 1-8.

Vargas, M., *et al.* (2013). Effect of long-term starvation conditions on polyphosphate- and glycogen-accumulating organisms. Bioresource Technology **127**: 126-131.

Vuono, D. C., *et al.*. (2015). Disturbance and temporal partitioning of the activated sludge metacommunity. The ISME journal, 9(2), 425-435.

Vuono, D. C., *et al.* (2016). rRNA gene expression of abundant and rare activated-sludge microorganisms and growth rate induced micropollutant removal. Environmental Science & Technology, 50(12), 6299-6309.

Wu, H., *et al.* (2016). Removal of methyl acrylate by ceramic-packed biotrickling filter and their response to bacterial community. Bioresource Technology, 209, 237-245.

Yan, S. and Wu, G. (2017). Reorganization of gene network for degradation of polycyclic aromatic hydrocarbons (PAHs) in Pseudomonas aeruginosa PAO1 under several conditions. Journal of Applied Genetics, 58(4), 545-563.

Yu, K. and Zhang, T. (2012). Metagenomic and Metatranscriptomic Analysis of Microbial Community Structure and Gene Expression of Activated Sludge. Plos One, 7(5).

Yu, K., *et al.* (2019). An integrated meta-omics approach reveals substrates involved in synergistic interactions in a bisphenol A (BPA)-degrading microbial community. Microbiome, 7(1), 1-13.

Zhang, T., *et al.* (2012). 454 Pyrosequencing reveals bacterial diversity of activated sludge from 14 sewage treatment plants. The ISME Journal 6(6), 1137-1147.

Zhang, W. *et al.* (2021). Microbial community and function evaluation in the start-up period of bioaugmented SBR fed with aniline wastewater. Bioresource Technology, 319, 124148.

Zhao, Y. A., *et al.* (2012). RAPSearch2: a fast and memory-efficient protein similarity search tool for next-generation sequencing data. Bioinformatics **28**(1): 125-126.

Zhu, L., *et al.* (2008). Formation and microbial community analysis of chloroanilines-degrading aerobic granules in the sequencing airlift bioreactor. Journal of Applied Microbiology **104**(1): 152-160.

Zhu, L., *et al.* (2014). Microbial community analysis for aerobic granular sludge reactor treating high-level 4-chloroaniline wastewater. International Journal of Environmental Science and Technology, 11(7), 1845-1854.

Figures and Figure Legends

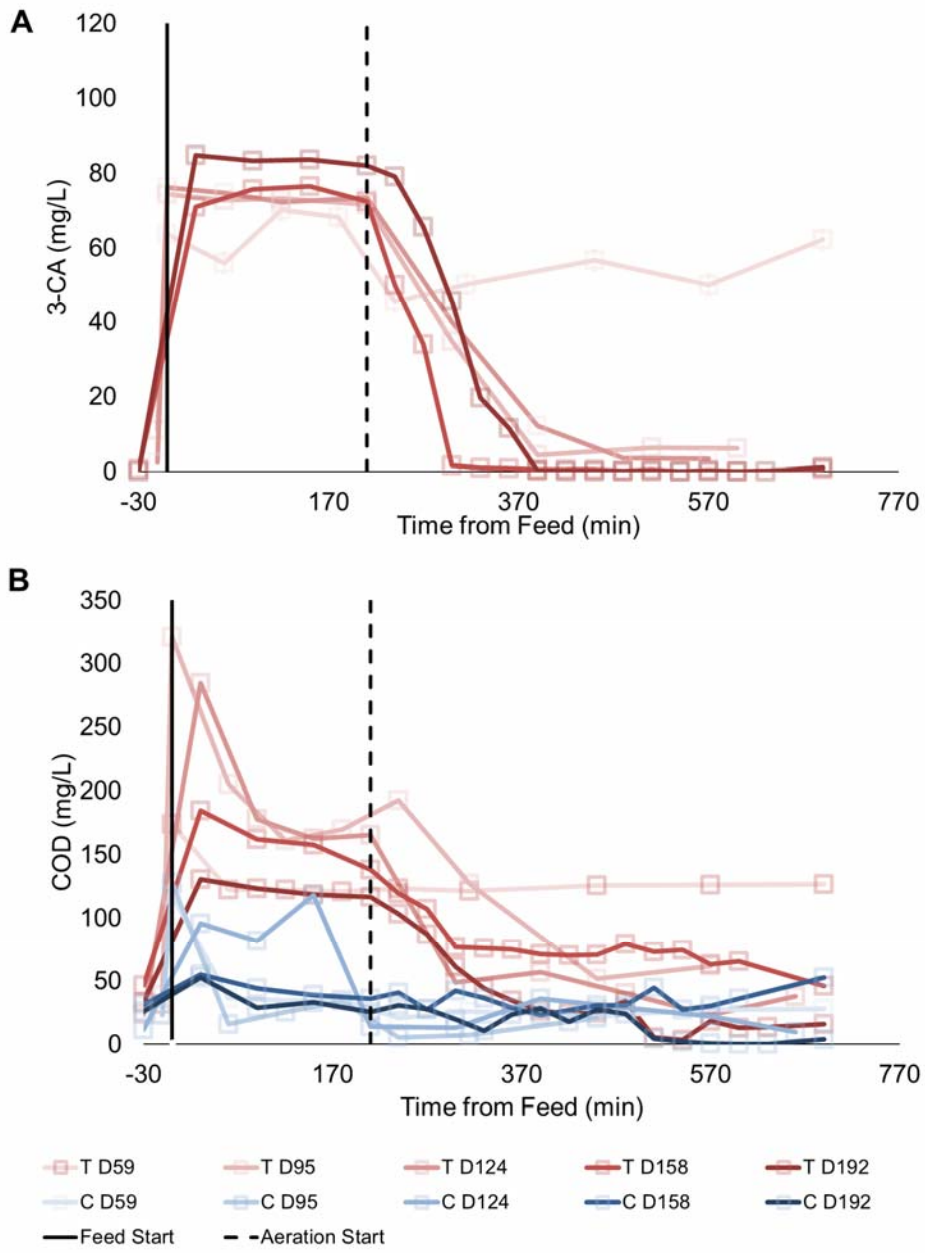

Figure 1. Average nutrient concentration profiles from five distinct days of the experiment showing degradation of COD and 3-CA over single 12-h cycles for all six reactors. The x-axes represent time from the commencement of feeding in min. The dotted vertical line (at x = 210 min) separates the anoxic and aerobic phases. Aeration began at 210 min. The y-axes represent (**A**) 3-CA, mg/L and (**B**) COD, mg/L. Data series in shades of blue represent control reactors (no 3-CA) and data series in shades of red represent treatment reactors (3-CA added), with decreasing brightness over time.

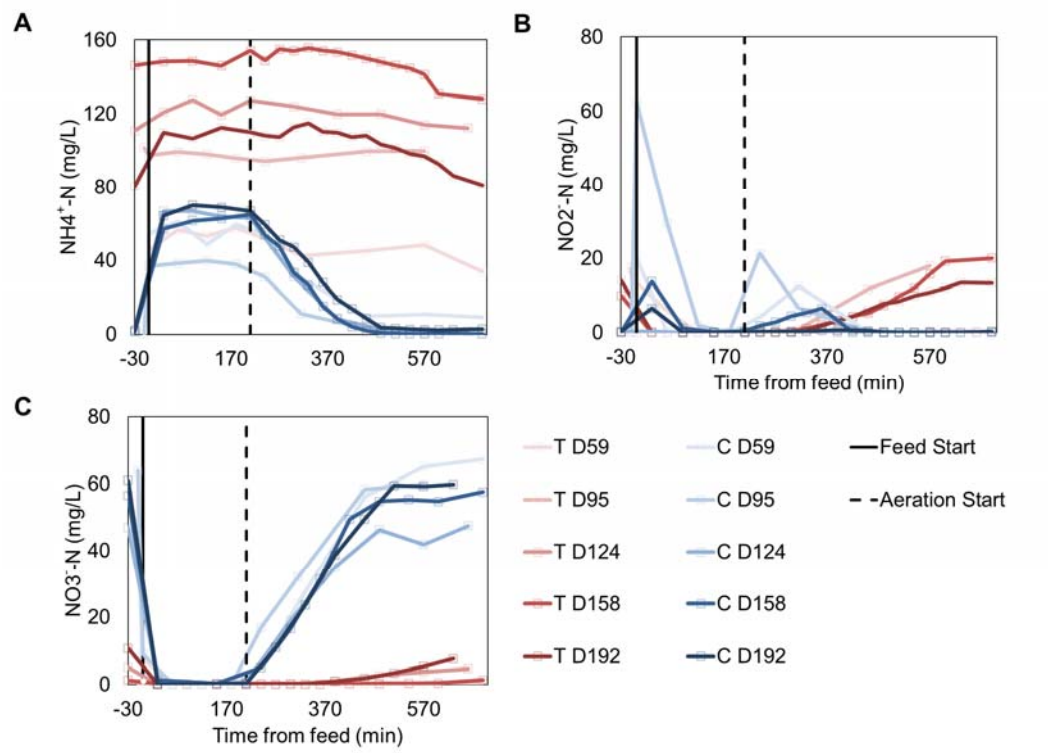

Figure 2. Average nutrient concentration profiles from five distinct days during the experiment showing nitrogen transformations over single 12-h cycles on all six reactors. The x-axes represent time from the commencement of feeding in min. The dotted vertical line (at x = 210 min) separates the anoxic and aerobic phases. Aeration began at 210 min. The y-axes represent (**A**) ammonium-nitrogen, mg/L and (**B**) nitrite-nitrogen, mg/L , and (**C**) nitrate-nitrogen, mg/L . Data series in shades of blue represent control reactors (no 3-CA) and data series in shades of red represent treatment reactors (3-CA added), with decreasing brightness over time.

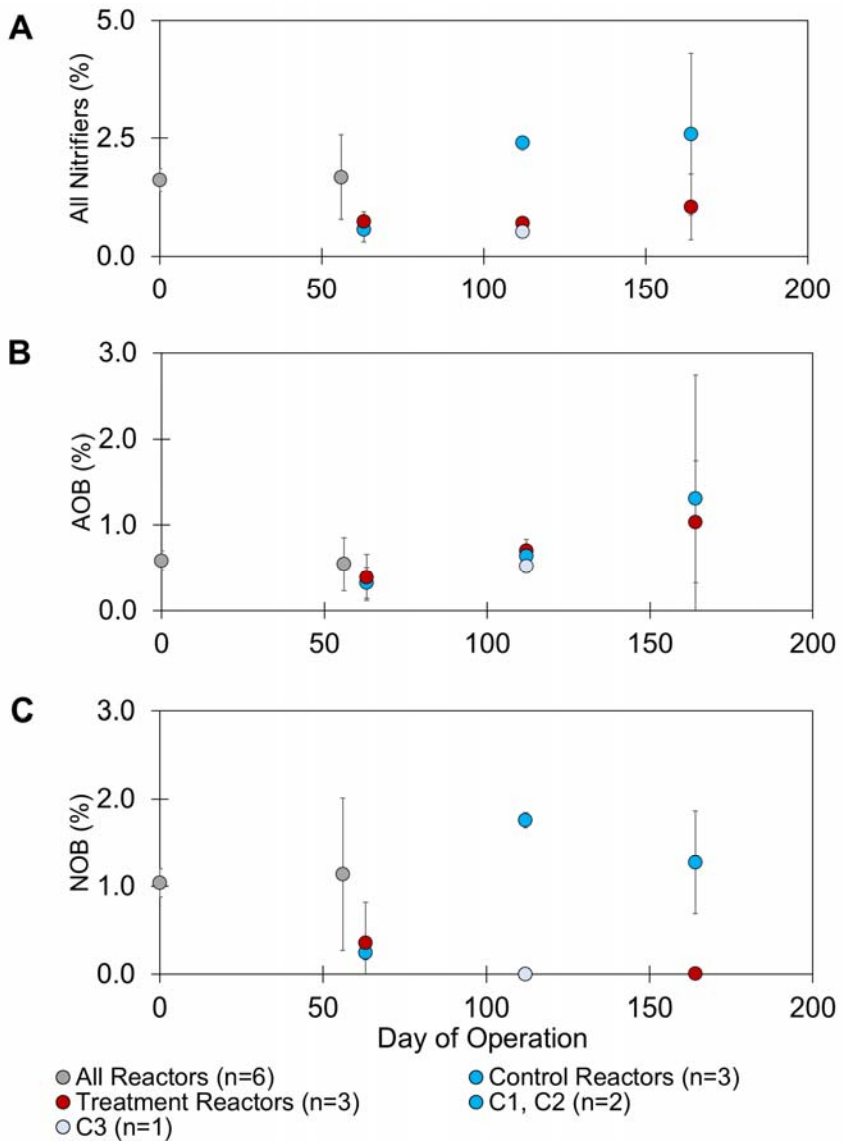

Figure 3. Changes in relative abundances of (A) total nitrifiers, (B) ammonia-oxidizing bacteria, and (C) nitrite oxidizing bacteria in control and treatment reactors over the course of the experiment, as determined from total normalized ASV counts from 16S rRNA amplicon sequencing data. Data points represent the mean of normalized read counts of the relevant nitrifier ASVs as a percentage of total normalized read counts of all ASVs from replicate reactors. Error bars represent one standard deviation of the mean. Note that reactor C3 on D112 is coloured differently because of its presumed divergence, due to exposure to 3-CA during a single cycle prior to this sample. Reactors C1 and C2 on D112 are coloured similarly to all three control reactors on other days.

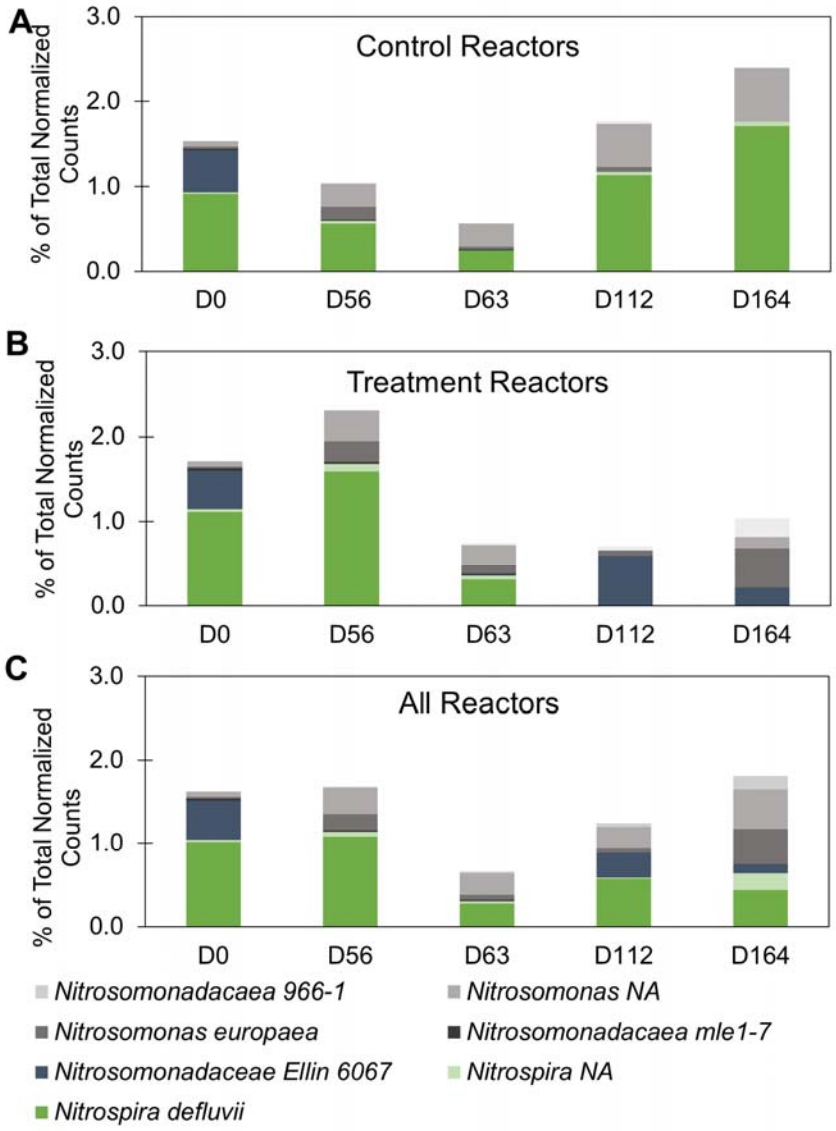

Figure 4. Changes in relative abundances of all detected nitrifier ASVs in (A) control reactors (no 3-CA; n = 3, except on D112 where C3 has been removed), (B) treatment reactors (3-CA added, n = 3), and (C) all reactors (n = 6), as determined from normalized ASV counts from 16S rRNA gene amplicon sequencing data.

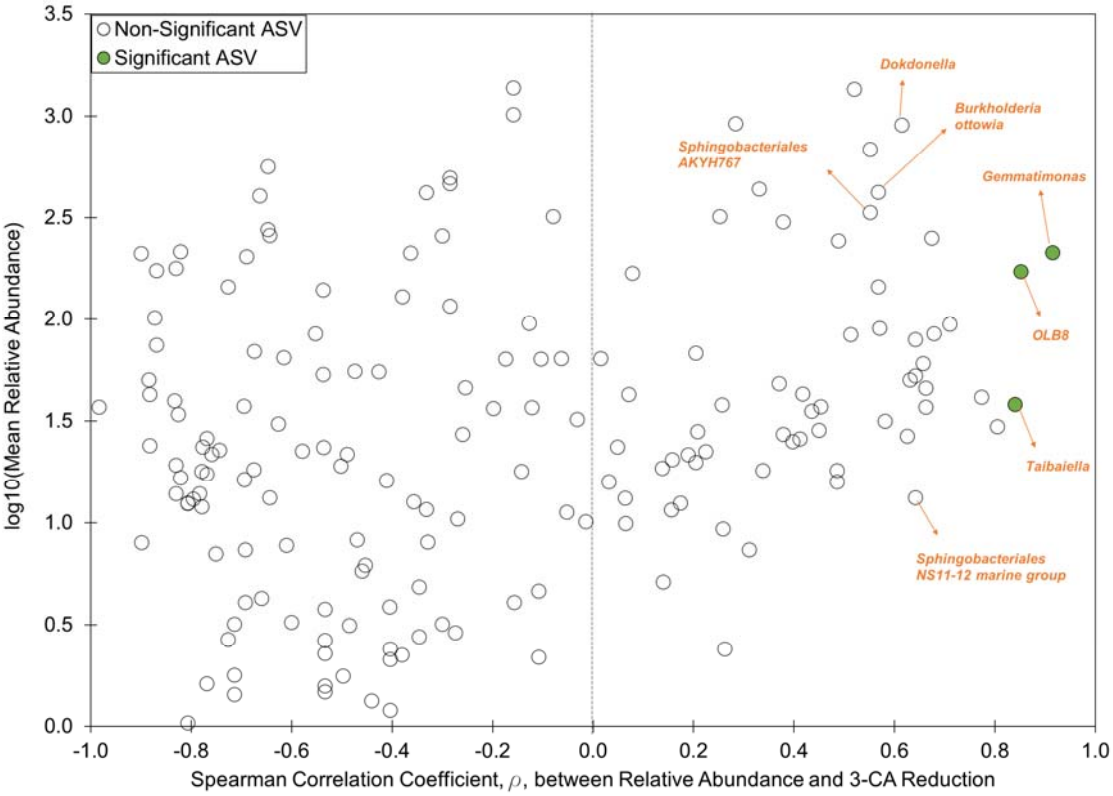

Figure 5. Relative abundances of the top 180 ASVs identified via 16S rRNA amplicon sequencing on D63, D112 and D163, plotted against the Spearman's Rank Order Correlation Coefficient of their respective relative abundances to 3-CA reduction in treatment reactors on D59, D110 and D171, respectively (n = 9). ASVs with significant correlation to 3-CA degradation (filled in data points) after a 10% FDR adjustment for multiple comparisons are identified by name, as are other ASVs with high correlation that were considered relevant to 3-CA degradation.

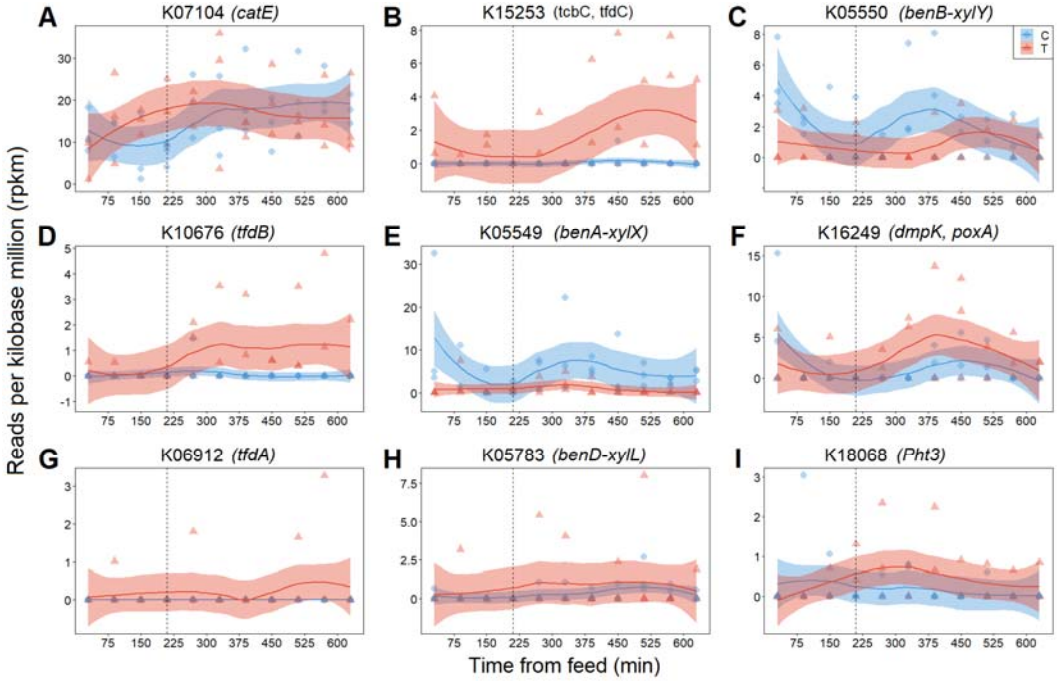

Figure 6. Average rpkm profiles of nine genes considered relevant to 3-CA degradation from which non-zero rpkm values were derived. rpkm profiles are shown over a single 12-h cycle on D171, averaged for the control (blue time series) and treatment (red time series) reactors for genes represented by KEGG orthologs K07104 (A), K15253 (B), K05550 (C), K10676 (D), K05549 (E), K16249 (F), K06912 (G), K05783 (H) and K18068 (I). The dotted vertical line (at x = 210 min) separates the anoxic and aerobic phases. Aeration began at 210 min. Lines display polynomial regression fitting, while shaded areas represent 95% confidence intervals.

Table 1. Major putative genes[1] involved in 3-CA degradation as identified from metagenomics and transcriptomics analyses.

KEGG Ortholog No.	Gene Name	Enzyme Name	Differential Enrichment ($D_z \geq 1.4$)[2]	Significant Differential Enrichment[2]	Differential Transcription[3]
Potential Upper Pathway Genes					
K05550	*benB-xylY*	Benzoate/toluate 1,2-dioxygenase subunit beta	Y	Y	N
K05549	*benA-xylX*	Benzoate/toluate 1,2-dioxygenase subunit alpha	Y	Y	N
K16268	*todC/bedC2/tcbAB*	Benzene/toluene/chlorobenzene dioxygenase subunit beta	Y	Y	N
K10676	*tfdB*	2,4-dichlorophenol 6-monooxygenase	Y	N	Y
K16249	*dmpK/poxA*	phenol/toluene 2-monooxygenase	Y	N	N
Potential Lower Pathway Genes					
K15253	*tfdC*	Chlorocatechol 1,2-dioxygenase	Y	N	Y
K07104	*catE*	Catechol 2,3-dioxygenase	Y	N	N

[1] The full list of putative genes analysed is provided in Table S1.
[2] Differential enrichment was assessed based on D_z analysis. Significant differential enrichment was assessed via a t-test of means of gene abundances between treatment and control reactors for genes with $D_z \geq 1.4$, and a 10% FDR correction for multiple comparisons. Metagenomics data from D176 were used for this differential enrichment assessment.
[3] Differential transcription was assessed using time series plots of the transcription levels of the gene as determined from transcriptomics data during a cycle on D171. A gene was assumed to be differentially transcribed if rpkm levels of a given gene were consistently higher in treatment reactors during the aerobic phase, as compared to levels in the anoxic phase and/or in control reactors.